

Comparative Study of Pure Mg and AZ91D as Sacrificial Anodes for Reinforced Cement Concrete Structures in Chloride Atmosphere

Yogesh Iyer Murthy ^{a*}, Sumit Gandhi ^b, Abhishek Kumar ^c

^a PhD Scholar, Department of Civil Engineering, Jaypee University of Engineering and Technology, Guna, India.

^b Associate Professor, Department of Civil Engineering, Jaypee University of Engineering and Technology, Guna, India.

^c Department of Applied Mechanics, Motilal Nehru National Institute of Technology, Allahabad-211001, India.

Received 14 February 2018; Accepted 10 August 2018

Abstract

Comparative study of the corrosion behavior of pure Magnesium and AZ91D anodes in reinforced cement concrete was undertaken in the present work. The steel reinforcements were kept in contact with these anodes electrochemically in chloride atmosphere and the half-cell potential drop was observed. Bare steel reinforcements were tied to the anodes and were also kept in high chloride atmosphere to test the mechanical properties. The yield stress and ultimate tensile stress were found to decrease by approximately 50MPa while the reduction in percentage elongation is approximately 25% for reinforcements tied to AZ91D and pure Mg at the end of 80 days compared to fresh steel reinforcement. The rate of corrosion of pure Mg was reportedly slightly higher compared to AZ91D due to the presence of inter-metallics as inferred through micro-graphs.


Keywords: Cathodic Protection; AZ91D; Mechanical Properties; Micro-Characterization; Inter-Metallics.

1. Introduction

The corrosion of steel reinforcement is one of the underlying factors which affect the durability of structure (Page CL). There are several factors which initiate corrosion, such as, ingress of free chloride ions, carbon dioxide, fluoride ions or sulphate ions. The concrete pore network, permeability, rate of ingress by diffusion or capillary suction are some factors (Ožbolt) which enhance the corrosion rate (Koleva) due to the above-mentioned ions. Amongst the agents of corrosion mentioned, chloride ions are the most important sources for the degradation of concrete (Escalante). (V.Kumar) (Song), especially in coastal regions. The ingress of chlorine causes the formation of HCl, which being a strong acid, reduces the pH of concrete. When the reduction in pH reaches a threshold value (typically < 8) (Broomfield), corrosion of steel reinforcements occur due to localized breakdown of the passivating film (Montemor).

Cathodic protection (CP) of reinforced cement concrete (RCC) structures has been in practice since decades (C.L. Page). This technique is widely used for structural integrity against corrosion in regions exposed to chloride atmosphere or extreme marine environment (Fuyong Cao). The underlying principle of CP technique is based on electro-chemical reaction involving the anodic dissolution of metal by providing electrons to the metal structure to be protected. The process of CP can be accomplished in two ways, viz. impressed current cathodic protection (ICCP) and galvanic coupling or sacrificial anoding of suitable material. The most commonly used anodes amongst the latter technique are pure Magnesium (Mg) (Fontana). Its low efficiency (~50%) is surpassed by the very high negative potential, which in turn provides high current output. The corrosion rate of Mg is high and hence, alloying is pursued. Amongst the alloys

* Corresponding author: yogesh.murthy@juet.ac.in

 <http://dx.doi.org/10.28991/cej-03091110>

➤ This is an open access article under the CC-BY license (<https://creativecommons.org/licenses/by/4.0/>).

© Authors retain all copyrights.

of Mg, AZ91D is a very commonly used alloy for CP. Although significant research could be found on the use of Mg and AZ91D for CP, very little work on the mechanical behavior of steel protected with these anodes and on the microstructural characterization of such anodes (Adeniyi) (Fan) (Zander). Additionally, not much work is reported on the systematic experimental investigation of macrocell corrosion of these anodes (Adeniyi) (Fuyong Cao). Based on the above discussion, it could be emphasized that there is a need for systematic investigation of Mg and AZ91D alloy anodes from micro to macro scale.

Thus, the primary focus of this research is to compare the ability of pure Mg and AZ91D in corrosion mitigation in RCC and to study the consequences of cathodic protection on the mechanical behavior of bare steel reinforcements in high chloride atmosphere. Further, microscopic examination of the corroded anodes is carried out to study the microstructure. A systematic analysis of the corrosion behavior of the anodes is expected to aid in selection of suitable anode under different conditions and also provide a comparative study of the two anodes.

2. Experimental Set-Up

The experiment was performed in two stages. Pure Mg and AZ91D anodes were first embedded in reinforced concrete slab and half-cell potential was measured up to 270 days. Next, bare steel reinforcements were fastened with anodes and placed in saturated solution of NaCl for 80 days. The detailed experimental set-up for both the cases is discussed below:

2.1. Reinforced Concrete Slab

Four reinforced cement concrete slabs of dimension $1000 \times 1000 \times 100$ mm were cast using 1:1.5:3 nominal mixes and a water to cement ratio of 0.45. All the slabs used 10 mm diameter steel reinforcements mat placed with a clear cover of 25 mm from all sides and with a center to center spacing of 190 mm. Figure 1 shows the schematic sketch of the reinforcement spacing. The surface area of steel reinforcement mat was found to be 1.884 m^2 . The reinforcements were treated with pickling solution in order to remove corrosion sites. Anodes 22 mm diameter and 250 mm long were centrally placed and tied intact to complete the electrochemical cell. Slab one and two were casted without NaCl and with 3.5% NaCl by weight of cement respectively using pure as cast, Mg anodes. Similarly, slab three and four were cast without NaCl and with 3.5% NaCl by weight of cement using AZ91D anode respectively. The notations for all the slabs are shown in Table 1. These slabs were constructed using tap water with specifications as shown in Table 2 on the same day, so as to maintain similar casting conditions.

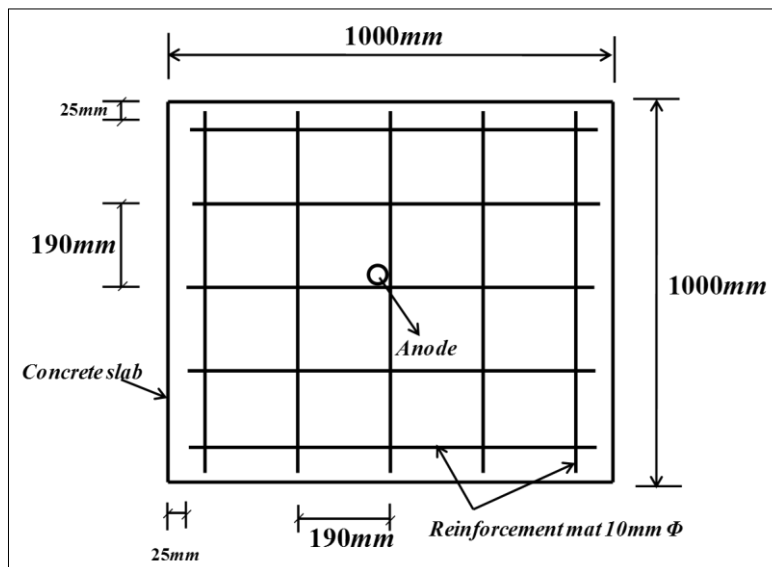


Figure 1. Detailing of reinforcement spacing and position of anodes for all four slabs

The process of construction of RCC slab is shown in Figure 2. Wooden formwork of dimension $1000 \times 1000 \times 150$ mm was used for casting as shown in Figure 2(a). The height of the slab was marked at 100 mm with marker. An impermeable sheet was spread at the bottom of the slab to prevent direct contact of fresh concrete with the flat ground so that water present in concrete does not interact with ground and water-cement ratio is maintained. Next, the reinforcement mat was prepared and conducting wire was wound rigidly over the reinforcement and the anode was tied intact at the center with the reinforcement. 75 mm thick cover blocks with 40 mm diameter made of cement mortar of 1:3 ratios were placed at the intersections of reinforcement so that a clear cover of 25 mm from the top is provided. Figure 2(b) shows the completed slab filled with fresh concrete while Figure 2(c) shows the concrete slab after curing for 28 days.

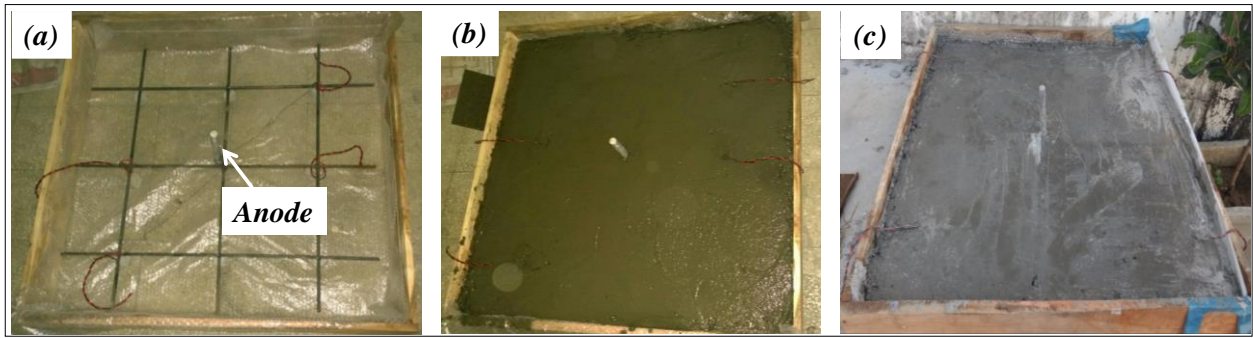


Figure 2. Experimental procedure for casting of RCC slabs

Table 1. Notation of different cases of Cathodic Protection

S.No.	Description	Notation
1	Without NaCl with pure Mg anode	CP0M
2	With 3.5% NaCl by weight of cement with pure Mg anode	CP35M
3	Without NaCl with AZ91D anode	CP0AZ91D
4	With 3.5% NaCl by weight of cement with Az91D anode	CP35AZ91D

The test for tap water was conducted strictly in accordance to IS: 10500:2012 (Specification, Indian Standard Drinking Water. "IS 10500.(2012)." Bureau of Indian Standards., 2012) and it was observed that the tap water consisted of 0.1 mg/l of free residual chlorine and 0.4 mg/l of fluoride ions. These free ions contribute to the conductivity of electrolyte, viz. concrete in this case. But since all the slabs were cast with same free chloride and fluoride content the effects of these ions are same in all cases and hence, innocuous.

Table 2. Tap water characteristics confirming IS: 10500:2012

S No.	Parameter	Value
1	Chloride	168mg/l
2	pH	7.6
3	Fluoride	0.4mg/l
4	Dissolved Oxygen	10.15mg/l
5	Chemical Oxygen Demand	0
6	Biological Oxygen Demand	0
7	Free Residual Chlorine	0.1mg/l

2.2. Test Set-Up for Bare Steel in Chloride Atmosphere

In order to further investigate the performance of pure Mg and AZ91D anodes on corrosion prevention of bare steel reinforcements three set of six steel reinforcements were tied together intact with centrally placed anode to complete the electrochemical cell. All the samples were dipped in high chloride atmosphere of 7.5% NaCl in tap water. Sample set one did not contain any anode; sample set two consisted of AZ91D anode while sample set three contained pure Mg anode. These samples were tested for weight loss, tensile strength and microstructure. The set-up consisted of a container $1 \times 1 \times 1$ m as shown in Figure 3. The bare steel reinforcements were selected from the same lot of steel so as to maintain uniform chemical composition and were treated with pickling solution to remove initial corrosion sites. It was ensured that the samples are kept vertical and undisturbed in the container. All the readings were taken on same days and at the same time to nullify the effect of variations in relative humidity and temperature.

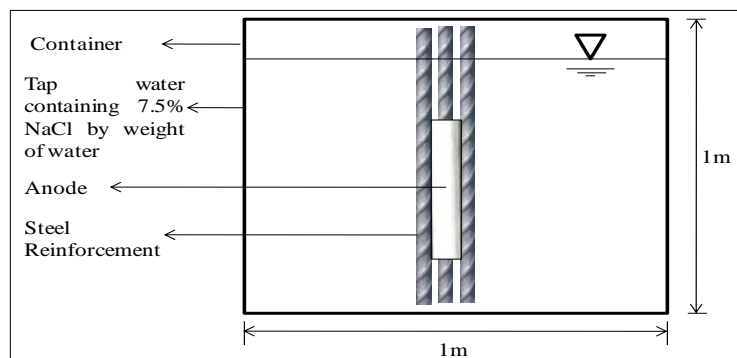


Figure 3. Schematic of set-up used to access the performance of anodes in high NaCl content atmosphere

2.3. Measurement Technique for Half Cell Potential

The measurement of the half-cell potential was done using the Standard Calomel Electrode (SCE). Half-cell potential is obtained as the potential difference with respect to a reference electrode (Elsener). The arrangement for this measurement is shown in Figure 4. The half-cell potential measurement is based on electrolytic continuity between reinforcement present in concrete, SCE in contact with the concrete surface and the potentiometer. In case of reinforced concrete slab, the transport of ions causes the electric conduction between reference electrode and concrete. For the establishment of proper electrolytic contact in concrete surface, wet fiber wick is placed between SCE and concrete surface to reduce the liquid junction potential between the two. The fiber wick was cleaned at regular intervals to prevent contamination of SCE.

3. Results and Discussion

3.1. Comparison of Potential of Reinforcement Embedded in Concrete for Slab without Anode, with Pure Mg Anode and with AZ91D

Figure 5 shows the variation of negative potential of the concrete slab with respect to Standard Calomel Electrode (SCE) at a distance of 10 cm from the anode for different days. In general, as expected, it could be found that as the number of days increase, the negative potential w.r.t. SCE decreases. Another obvious result is that the slabs not having NaCl have relatively less negative potential.

Further, among the two slabs without NaCl, it is found that cathodic protection of slab containing AZ91D (i.e. CP35AZ91D) without NaCl has the least negative potential. This could be attributed the fact that the interaction of Al, Mg and Zn leads to formation of various intermetallics, which have different electrochemical potential compared to pure Mg. Thus, the overall electrochemical potential of the alloy is less, leading to slower rate of corrosion.

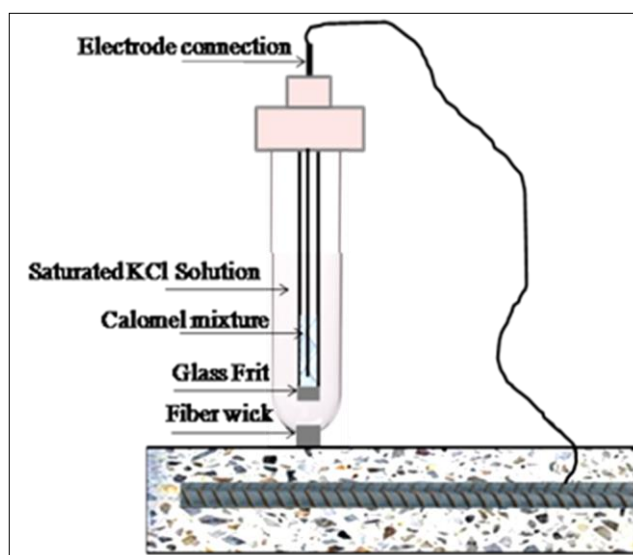
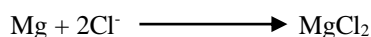


Figure 4. Experimental set-up and measurement technique

Another interesting observation is the increasing trend of negative potential during the 50th to 100th day. Since the slabs were exposed to atmosphere, the ingress of water during monsoon, led to increased conductivity of the slab, leading to higher negative potential values.

The negative potential of slab CP35M reduces drastically after nearly 175 days. This could be possible due to rapid consumption of free chloride ions by pure Mg according to the following reaction:



This notion is further augmented by the fact that as the number of days increased several radial cracks along with white crystalline deposits could be observed around the pure Mg anode which is due to increased volume of MgCl_2 . The chemical composition of the crystalline white deposits were analyzed and it was confirmed that the deposits typically consisted of MgCl_2 and Cl_2 , the later being in very less quantity, probably deposited due to condensation.

It is also observed that by the 270th day, the negative potential of all slabs, except CP35AZ91D are in the range of -200 to -300mV w.r.t. SCE. Much higher negative potentials of the slab containing 3.5% NaCl and AZ91D anode further augments the proposition of the formation of intermetallics and hence reduced rates of interaction with Cl^- ions.

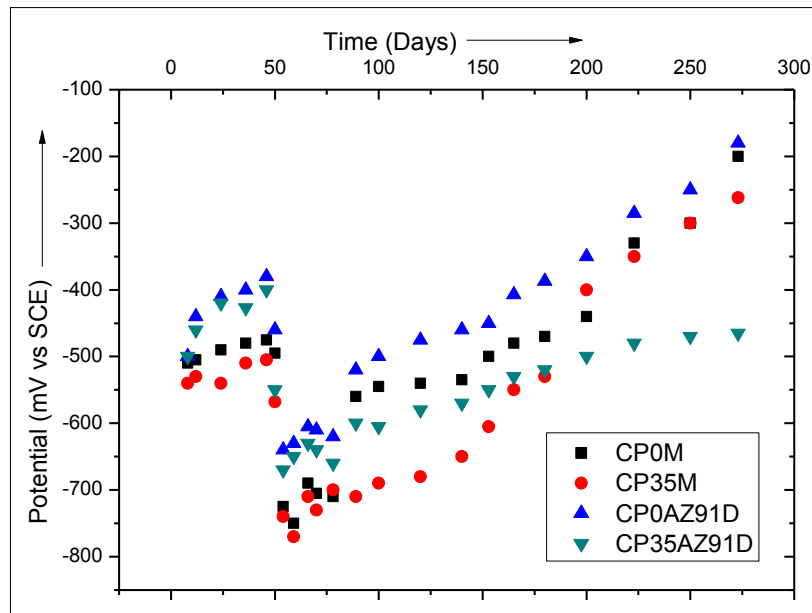


Figure 5. Variation of negative potential of slab w.r.t. SCE for various days at a distance of 10cm from anodes for all four cases

3.2. Comparison of Tensile Strength in Bare Steel Bars with AZ91D and Pure Mg Anode

Three sets of six bare steel reinforcements, 950 mm long and 10 mm diameter were tied closely with centrally placed anodes, 22 mm diameter and 250 mm long. The cross section for the set-up is as shown in Figure 6. The steel reinforcements were maintained at a height of 200 mm from the bottom, in order to ensure partial immersion and were kept undisturbed. The temperature of the set-up was maintained at 27°C. Steel rods were taken out on the 20th, 40th, 60th and 80th days and tested for tensile strength in a 100 ton Universal Testing Machine for yield stress, ultimate stress and % elongation. The results for tensile test of AZ91D and pure Mg are presented in Figures 7(a) and 7(b) respectively.

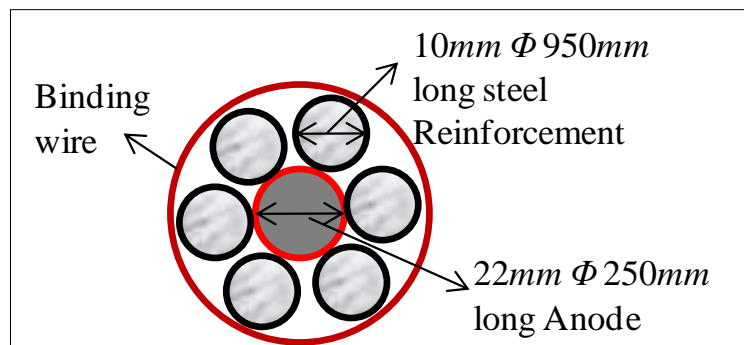


Figure 6. Cross-section of set-up for the test of bare steel reinforcement

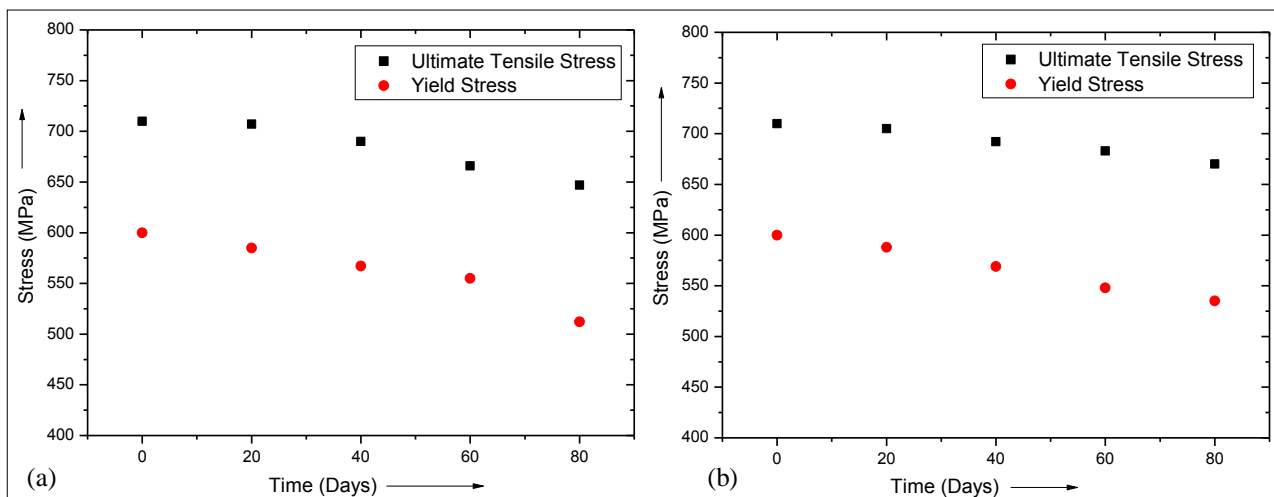


Figure 7. Yield stress and Ultimate tensile stress of steel reinforcement in MPa under high Chloride (7.5%) atmosphere with (a) AZ91D and (b) pure Mg

From Figure 7 it could be inferred that compared to fresh steel reinforcement, in both the cases there is a drop in Yield stress and Ultimate tensile stress by nearly 50MPa at the end of 80 days. The drop in percentage elongation for these reinforcements is shown in Figure 8. At the end of the test period, it is found that this reduction in percentage elongation is approximately 25% for reinforcements tied to AZ91D and pure Mg; although, reduction in case of AZ91D is observed to be slightly higher compared to pure Mg anodes.

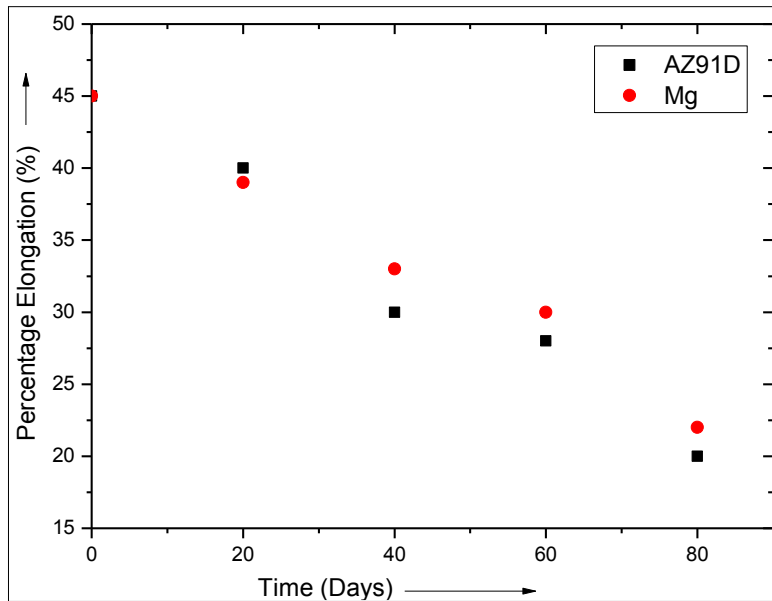


Figure 8. Percentage elongation of steel reinforcement under high Chloride (7.5%) atmosphere with AZ91D and pure Mg

3.3. Comparison of Rate of Corrosion in Bare Steel Bars with AZ91D and with Pure Mg Anode

The rate of corrosion in both the cases is evaluated and presented in Table 3 using the standard expression as mentioned below:

$$\text{Rate of Corrosion (mm/yr)} = 87.6 \times \frac{W}{DAT}$$

Where

W = Weight loss in milligrams

D = Density of steel (obtained as 7.89 g/cc)

A = Area of steel (cm²)

T = Time of exposure to chloride atmosphere in Hours

Table 3. Rate of corrosion (mm/yr)

S.No.	Time (Days)	Pure Mg	AZ91D
1	0	0	0
2	20	0.127819	0.10091
3	40	0.08981	0.077364
4	60	0.069516	0.061667
5	80	0.0555	0.052978

One of the obvious results observed from Table 3 is that the rate of corrosion is faster at the beginning and slower as the time proceeds. Also, the rate of corrosion of pure Mg is slightly higher compared to AZ91D.

3.4. Microstructure of Corroded Anodes (Mg/ AZ91D) vs Un-Corroded

The anodes from the concrete was taken after 270 days of embedment and observed microscopically using Hitachi S-3400N SEM equipped with Energy Dispersive Spectroscopy (EDS). The analysis of samples was carried out with a 2 µm probe diameter, 10 kV accelerating voltage and 50 nA probe current. The error of the SEM measurements is estimated to be about ± 2 at. %.

3.4.1. Microstructure of Pure Mg

Figure 9 (a-d) reveals the backscattered electron images (BSEI) of corroded and un-corroded parts of pure Mg after 270 days of embedment in concrete, with gradually increased magnification of the area of interest to systematically understand the features of the anode. Figure 9 (a) shows the junction of corroded and un-corroded regions of the anode.

Three distinct features could be observed in the micrograph, namely, white, grey and spots of darker shade of grey. EDS spot analysis was carried out to deduce the composition of these features. The spectral composition of white layer was found to be pure Mg, the grey layer consisted of MgO, while point analysis of the dark grey features confirmed the formation of MgCl₂ in the corroded region. Figure 9 (b) and 9 (d) show the magnified images of the corroded regions, while Figure 9 (c) shows the un-corroded region. It could be seen that there are grey regions in the pure Mg due to formation of MgO.

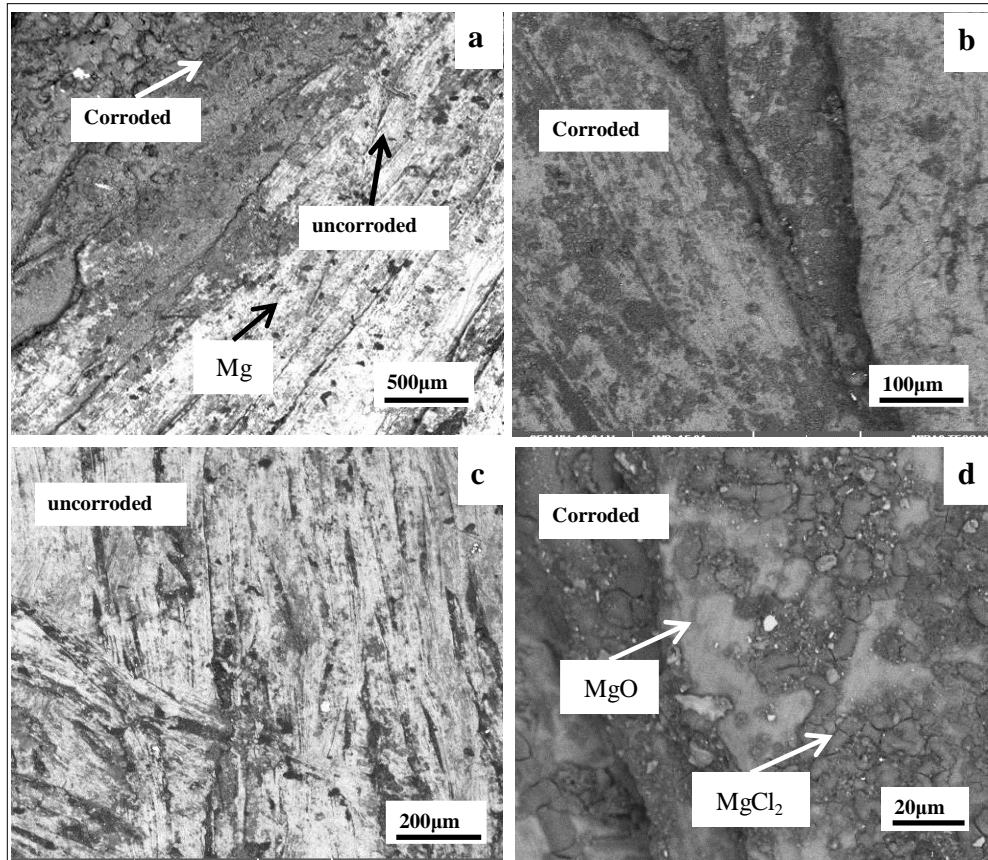


Figure 9 (a-d). BSEI of corroded and un-corroded parts of pure Mg

Further, Figure 10 shows the area analysis of 400µm of corroded part of pure Mg. The area analysis affirms the findings of EDS spot analysis, showing the presence of MgCl₂ and MgO.

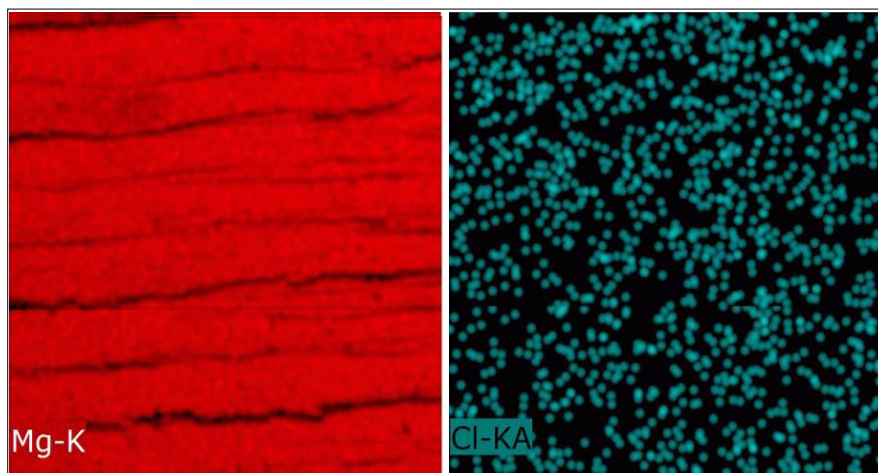


Figure 10. Area analysis of corroded part of pure Mg

3.4.2. Microstructure of AZ91D

BSEI of the unpolished as-cast alloy revealed that the macro-scopically smooth alloy anode actually consisted of ridges or protrusions (Figure 11 (a)). The EDS spot analysis revealed that these ridges were composed of MgO roughly 20 µm long.

The micro-structure of polished un-corroded as-cast sample of AZ91D is shown in Figure 11 (b). The objective to analyze the micro-structure of polished sample was to understand the internal structure of the alloy. It consists of Mg matrix and inter-metallics with well developed primary dendrites distributed along the α -Mg grain boundaries. The inter-metallics consist of $Mg_{17}Al_{12}$ (dark grey) and $Al_2Mg_5Zn_2$ (light Grey).

Figure 11(c) shows the BSEI of the corroded AZ91D alloy after 270 days of embedment. It consists of irregular oxide nodules (primarily MgO) of varying sizes ranging from 5-40 μm formed due to oxidation of α -Mg matrix and craters of $MgCl_2$ along with the matrix phase. The oxide nodules were formed preferentially at grain boundaries, while craters of $MgCl_2$ were randomly distributed.

It could be observed that $Mg_{17}Al_{12}$ phase acts as a barrier as well as a potential site for cathodic reaction. Similar observations were reported by Jonsson and Perrson. (Jönsson). Further, area analysis of 400 μm , Figure 11 (d) of sample shows the findings discussed above pictographically.

From the 100 μm BSEI of the corroded AZ91D Figure 12 it is seen that crevices were formed along the grain boundaries which lead to the following conclusions:

1. The Mg matrix gets oxidized to MgO or interacts with chloride forming $MgCl_2$, both of which have higher volume, leading to expansion of the matrix and chipping off thereafter.
2. The electro-chemical potential of the inter-metallics is lower compared to pure Mg as the chloride ions have preferential interaction with Mg. Thus, the pure Mg matrix acts as “active-sites” for interaction, while inter-metallics being dormant sites. Consequently, the corrosion rate of AZ91D is lower compared to pure Mg.

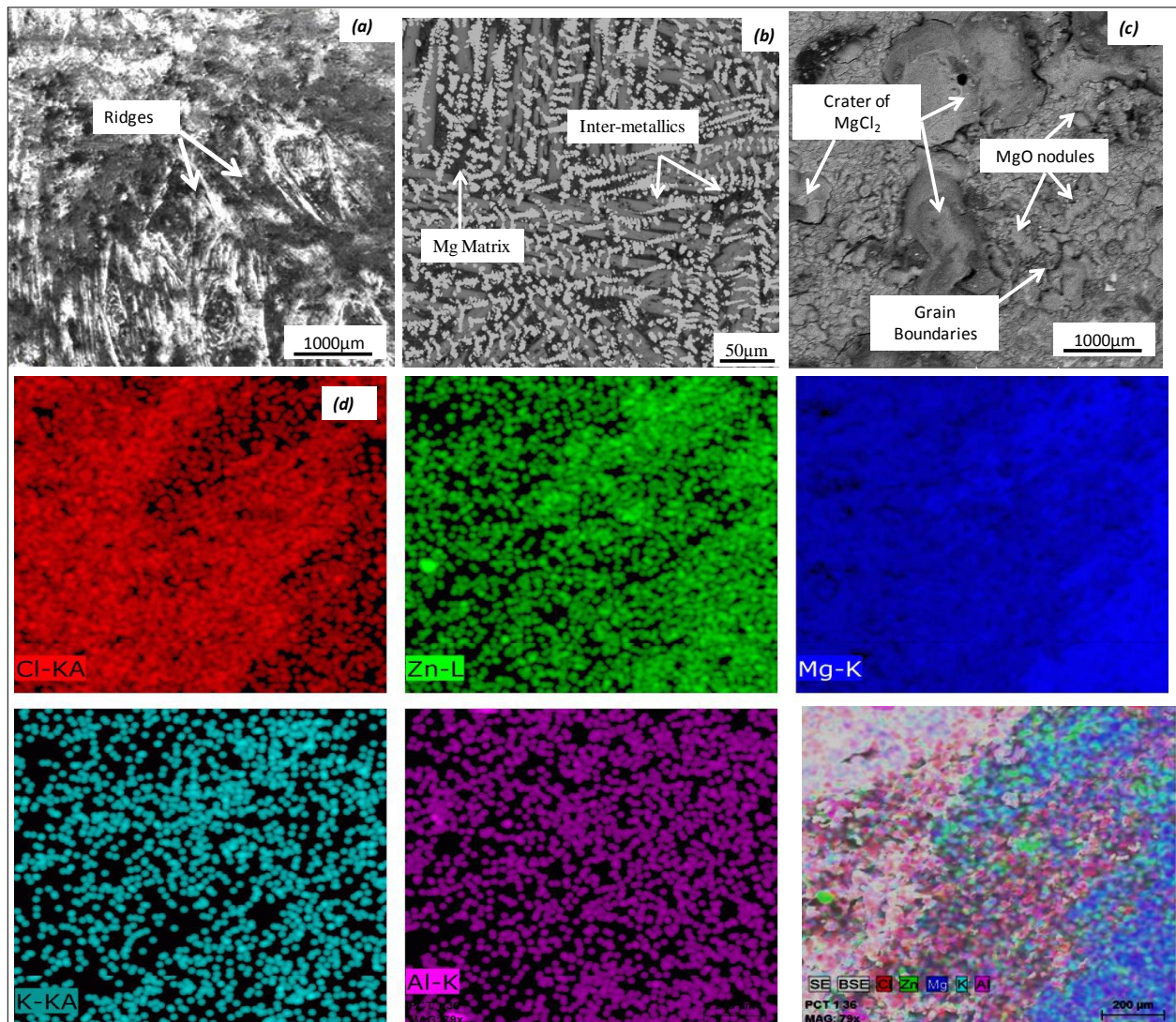


Figure 11. (a) BSEI of unpolished as-cast AZ91D, (b) BSEI of polished as-cast AZ91D, (c) BSEI of the corroded AZ91D alloy after 270 days of embedment and (d) Area analysis of corroded part of AZ91D

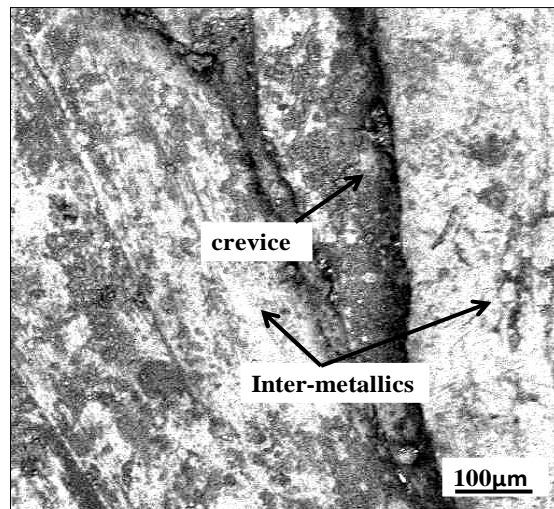


Figure 12. BSEI of corroded AZ91D showing crevices

Thus, it is seen that the process of corrosion of pure Mg and AZ91D is largely different on microscopic scale. The reduced rate of corrosion is also compared mathematically in Table 3.

4. Conclusion

In the current work, a systematic study was undertaken to investigate the mechanical properties of steel in electrochemical contact with pure Mg and AZ91D anodes using concrete with 3.5% NaCl by weight of cement and using bare steel in 7.5% NaCl dissolved in tap water. The potential of steel embedded in concrete with both the anodes showed a drop in negative potential w.r.t. SCE as the days increased. Relative humidity and temperature were found to influence the half-cell potential readings. The yield stress and ultimate tensile stress were found to decrease by approximately 50MPa while the reduction in percentage elongation is approximately 25% for reinforcements tied to AZ91D and pure Mg at the end of 80 days compared to fresh steel reinforcement. The mechanical properties of steel coupled with both the anodes showed similar results but the rate of corrosion of pure Mg was reportedly slightly higher compared to AZ91D due to the presence of inter-metallics as inferred through micro-graphs.

5. References

- [1] Page, C. L., and K. W. J. Treadaway. "Aspects of the electrochemistry of steel in concrete." *Nature* 297, no. 5862 (1982): 109.
- [2] Ožbolt, J., G. Balabanić, G. Periškić, and M. Kušter. "Modelling the Effect of Damage on Transport Processes in Concrete." *Construction and Building Materials* 24, no. 9 (September 2010): 1638–1648. doi:10.1016/j.conbuildmat.2010.02.028.
- [3] Koleva, D. A., J. H. W. de Wit, K. van Breugel, Z. F. Lodhi, and E. van Westing. "Investigation of Corrosion and Cathodic Protection in Reinforced Concrete." *Journal of The Electrochemical Society* 154, no. 4 (2007): P52. doi:10.1149/1.2436609.
- [4] Escalante, Edward, and Satoshi Itō. A bibliography on the corrosion and protection of steel in concrete. No. 548-551. Dept. of Commerce, Office of the Assistant Secretary of Commerce for Science and Technology, National Bureau of Standards: for sale by the Supt. of Docs., US Govt. Print. Off., 1979.
- [5] Kumar, V. Protection of steel reinforcement for concrete-A review. (1998): 317-358.
- [6] Song, Ha-Won, and Velu Saraswathy. "Corrosion monitoring of reinforced concrete structures-A." *Int. J. Electrochem. Sci* 2 (2007): 1-28.
- [7] Broomfield, J. *Corrosion of Steel in Concrete: Understanding, Investigation and Repair*. E & FN Spon. London, 1997.
- [8] Montemor, M.F., A.M.P Simões, and M.G.S Ferreira. "Chloride-Induced Corrosion on Reinforcing Steel: From the Fundamentals to the Monitoring Techniques." *Cement and Concrete Composites* 25, no. 4-5 (May 2003): 491–502. doi:10.1016/s0958-9465(02)00089-6.
- [9] Page, C. L. "Mechanism of corrosion protection in reinforced concrete marine structures." *Nature* 258, no. 5535 (1975): 514.
- [10] Cao, Fuyong, Guang-Ling Song, and Andrej Atrons. "Corrosion and Passivation of Magnesium Alloys." *Corrosion Science* 111 (October 2016): 835–845. doi:10.1016/j.corsci.2016.05.041.
- [11] Fontana, M. G. *Corrosion engineering*. Tata McGraw-Hill Education., 2005.
- [12] Adeniyi, Ayodele Samuel, and Mary Ajimegoh Awotunde. "Corrosion Susceptibility of a 0.35%C Steel in Seawater Electrolyte Using the Electrochemical Method." *International Journal of Engineering Research in Africa* 27 (December 2016): 20–26. doi:10.4028/www.scientific.net/jera.27.20.
- [13] Fan, Z., G. Liu, and Y. Wang. "Microstructure and Mechanical Properties of Rheo-Diecast AZ91D Magnesium Alloy." *Journal*

of Materials Science 41, no. 12 (April 21, 2006): 3631–3644. doi:10.1007/s10853-006-6248-x.

[14] Zander, Daniela, and Christian Schnatterer. "The Influence of Manufacturing Processes on the Microstructure and Corrosion of the AZ91D Magnesium Alloy Evaluated Using a Computational Image Analysis." *Corrosion Science* 98 (September 2015): 291–303. doi:10.1016/j.corsci.2015.05.032.

[15] Specification, Indian Standard Drinking Water. "IS 10500.(2012). Bureau of Indian Standards ." 2012.

[16] Elsener, B., C. Andrade, J. Gulikers, R. Polder, and M. Raupach. "Half-Cell Potential measurements—Potential Mapping on Reinforced Concrete Structures." *Materials and Structures* 36, no. 7 (August 2003): 461–471. doi:10.1007/bf02481526.

[17] Jönsson, Martin, and Dan Persson. "The Influence of the Microstructure on the Atmospheric Corrosion Behaviour of Magnesium Alloys AZ91D and AM50." *Corrosion Science* 52, no. 3 (March 2010): 1077–1085. doi:10.1016/j.corsci.2009.11.036.